Materials Science-Poland, Vol. 24, No. 1, 2006

$Bi_8V_2O_{17}$ – a stable phase in the Bi_2O_3–V_2O_5 system

W. WROBEL[1*], F. KROK[1], I. ABRAHAMS[2],
A. KOZANECKA-SZMIGIEL[1], M. MALYS[1], S. C. M. CHAN[2], J. R. DYGAS[1]

[1]Faculty of Physics, Warsaw University of Technology, ul. Koszykowa 75, 00-662, Warsaw, Poland

[2]Centre for Materials Research, Department of Chemistry, Queen Mary,
University of London, Mile End Road, London E1 4NS, United Kingdom

$Bi_8V_2O_{17}$ is commonly observed as an intermediate phase in the synthesis of compounds in ternary systems of the type Bi_2O_3–V_2O_5–Me_xO_y. It is also seen as an end product at particular compositions in these systems. A rhombohedral substructure model for this phase is presented along with electrical parameters. Evidence from the Arrhenius plot suggests a phase transition at around 550 °C. The existence of a limited solid solution of $Bi_8V_2O_{17}$ with ZrO_2 is also discussed.

Key words: *bismuth vanadate; oxide ion conductor; electrical conductivity; crystal structure*

1. Introduction

The Bi_2O_3–V_2O_5 system has attracted much attention in recent years. A number of phases have been identified in this binary system, including $BiVO_4$ [1, 2], $Bi_4V_2O_{11}$ [3], $Bi_{3.5}V_{1.2}O_{8.25}$ [4], $Bi_{23}V_2O_{44.5}$ [5] and $Bi_8V_2O_{17}$ [6]. While much research has gone into the orthovanadate phase $BiVO_4$, particularly regarding its catalytic properties (see e.g. [7]) and $Bi_4V_2O_{11}$ which is the parent compound of the BIMEVOX family of solid electrolytes [8], little attention has been paid to the other phases in this binary system.

$Bi_8V_2O_{17}$ is commonly observed as an intermediate phase in the synthesis of compositions in ternary systems of the type Bi_2O_3–V_2O_5–Me_xO_y [9]. This compound also appears as a final product of reaction in these systems for particular compositions (eg., $Bi_2Zr_xV_{1-x}O_{5.5-(x/2)}$ and $Bi_2Mg_xV_{1-x}O_{5.5-(3x/2)}$, x = 0.50) [10–12]. Here we present a study of the structure and electrical conductivity of $Bi_8V_2O_{17}$.

*Corresponding author, e-mail: wrobel@if.pw.edu.pl

2. Experimental

Preparations. Polycrystalline $Bi_8V_2O_{17}$ and samples of general formulae $Bi_2Zr_xV_{1-x}O_{5.5-(x/2)}$ ($0.20 \le x \le 0.50$) and $Bi_2Mg_xV_{1-x}O_{5.5-(3x/2)}$, $x = 0.50$, were prepared by standard solid-state methods. Appropriate amounts of Bi_2O_3 (Aldrich, 99.9%), V_2O_5 (ABCR, 99.5%), ZrO_2 (Aldrich, 99.5%) and MgO (POCh, 99,5%) were ground together as a toluene paste using a planetary ball mill. The dried powder was heated in a platinum crucible at 650 °C for 12 h. After cooling, the ground powder was pelletised and subjected to isostatic pressing at the pressure of 400 MPa. Pellets were sintered at 840 °C for 10 h and subsequently slow cooled in air to room temperature over 12 h.

Single crystals of $Bi_8V_2O_{17}$ were prepared by slow cooling a melt of appropriate starting materials. Bi_2O_3 and V_2O_5 were ground together in ethanol using an agate mortar and pestle. The dried mixture was heated at 650 °C for 10 h followed by subsequent heating at 800 °C for 20 h. Melting was carried out at 900 °C and the sample was kept at this temperature for 40 h before slow cooling in air to room temperature over 24 h. A single crystal of dimensions $0.15 \times 0.15 \times 0.12$ mm^3 was extracted from the cooled melt for diffraction studies.

Electrical measurements. Electrical parameters were determined by ac impedance spectroscopy up to ca. 800 °C using a fully automated Solartron 1255/1286 system in the frequency range from 1 Hz to 5×10^5 Hz. Samples for impedance measurements were prepared as rectangular blocks (ca. $6 \times 3 \times 3$ mm^3) cut from slowly cooled sintered pellets using a diamond saw. Platinum electrodes were sputtered by cathodic discharge. Impedance spectra were recorded automatically over two cycles of heating and cooling at programmed temperatures after 15 min of temperature stabilisation. Impedance at every frequency was measured repeatedly until consistency was achieved or a maximum number of 25 repeats had been reached. In addition, impedance at selected frequencies was measured before and after each spectral collection in order to determine the extent of drift. Where the summed differences exceeded a preset tolerance of 2%, the process was repeated.

Crystallography. Single-crystal X-ray intensity data were collected on an Enraf-Nonius CAD-4 diffractometer using MoK_α radiation (λ = 0.71073 Å) with ω–2θ scans at 20(2) °C. Data for 176 reflections were collected with 38 independent reflections in rhombohedral symmetry with $I > 2\sigma(I)$. The data were corrected for the Lorentz and polarization factors and corrected for absorption by empirical methods (Ψ-scan) [13]. The structure was solved by direct methods using SHELXS-97 [14] and refined on F^2 by full matrix least squares using SHELXL-97 [14]. Anisotropic thermal parameters were refined for all atoms. WINGX [15] was used to prepare material for publication. Crystal and refinement parameters for $Bi_8V_2O_{17}$ are summarised in Table 1.

A high resolution X-ray powder diffraction pattern was collected for pure $Bi_8V_2O_{17}$ at room temperature using an INEL CPS-120 fixed position sensitive detector system on an Enraf-Nonius FR590 X-ray generator. The curved position sensitive

detector allows simultaneous data collection in 4096 bins over 0° to 120° in 2θ. The sample was mounted on a Si-711 cut crystal and data collected in the 2θ range 0–120°, using Ge 111 monochromated CuKα_1 radiation (λ = 1.54056 Å), in fixed flat-plate geometry with the incident beam striking the sample holder at the angle of between 2° to 5°. Data were collected for a total scan time of 80 min. High temperature X-ray powder diffraction data were collected on $Bi_8V_2O_{17}$ at 700 °C on a Philips X'Pert X-ray diffractometer using graphite monochromated CuK$_\alpha$ radiation (λ_1 = 1.54056 Å and λ_2 = 1.54439 Å) with an Anton-Paar HTK 1200 high-temperature camera. Data were collected in flat plate $\theta/2\theta$ geometry on a Pt sample holder. Calibration was carried out with an external Si standard. Measurements suitable for Rietveld analysis were performed in the 2θ range 10–110°, in steps of 0.02°, with a scan time of 10 s per step. Unit cell dimensions and structural parameters were refined by Rietveld whole profile fitting using the program GSAS [16]. The single crystal derived parameters for $Bi_8V_2O_{17}$ were used as a starting model.

Table 1. Crystal and refinement parameters for $Bi_8V_2O_{17}$ substructure

Empirical formula	$Bi_{0.80}V_{0.20}O_{1.70}$
Formula weight	204.57
Temperature	293(2) K
Wavelength	0.71073 Å
Crystal system	trigonal
Space group	$R\bar{3}m$
Unit cell dimensions	a = 3.815(4) Å, α = 90° b = 3.815(4) Å, β = 90° c = 9.990(8) Å, γ = 120°
Volume	125.9(2) Å^3
Z	3
Density (calculated)	8.093 mg/m^3
Absorption coefficient	84.663 mm^{-1}
F(000)	254
Crystal size	0.15 × 015 × 0.12 mm^3
Θ range for data collection	6.13–24.56°
Reflections collected	176
Independent reflections	38 (R(int) = 0.2537)
Final R indices (I > 2sigma(I)]	R1 = 0.0479, wR2 = 0.1071
R indices (all data)	R1 = 0.0479, wR2 = 0.1071
Extinction coefficient	0.002(8)
Largest diff. max. and min.	2.652 and –1.460 e.Å^{-3}

X-ray powder diffraction data were collected on $Bi_2Zr_xV_{1-x}O_{5.5-(x/2)}$ and $Bi_2Mg_xV_{1-x}O_{5.5-(3x/2)}$ samples at room temperature on an automated Philips PW1050/30 X-ray diffractometer, using Ni filtered CuKα radiation (λ = 1.5418 Å). Data were collected in flat plate $\theta/2\theta$ geometry in the 2θ range 5–120°, in steps of 0.02, with scan times of 10s per step. Calibration was carried out with an external Si standard. Unit cell pa-

rameters were refined using a multiple phase refinement with the program GSAS [16]. The structures of γ-BICOVOX [17], ZrO_2 [18] and the single crystal derived parameters for $Bi_8V_2O_{17}$ were used as initial models in structure refinement.

Thermal Analysis. Differential thermal analysis was carried out using a Perkin Elmer DTA 7 apparatus at the heating/cooling rate of 10 °C·min^{-1} over an approximate temperature range 25–800 °C.

3. Results and discussion

The refined atomic parameters for the rhombohedral model for $Bi_8V_2O_{17}$ derived from the single crystal analysis are given in Table 2, along with significant contact distances. In this model, Bi and V share the 3*a* position (0, 0, 0) with oxide ions partially occupying the 6*c* position (–1/3, 1/3, 0.92). The fitted X-ray diffraction pattern

Table 2. Refined atom positions parameters and significant contact distances in the $Bi_8V_2O_{17}$ substructure. Estimated standard deviations are given in parentheses

Atom positions coordinates						
Atom	Site	x	y	z	Occ.	U_{eqv} (Å^2)
Bi/V	3a	0.0(–)	0.0(–)	0.0(–)	0.8/0.2(–)	0.0040(2)
O	6c	–0.3333(–)	0.3333(–)	0.092(13)	0.85(–)	0.031(19)

Anisotropic thermal parameters (Å^2)						
Atom	U_{11}	U_{22}	U_{33}	U_{23}	U_{13}	U_{12}
Bi/V	0.0043(3)	0.0043(3)	0.0034(2)	0.0(–)	0.0(–)	0.0022(1)
O	0.04(3)	0.04(3)	0.010(6)	0.0(–)	0.0(–)	0.021(15)

Contact distances (Å)	
Bi/V–O	2.39(5) Å × 6
Bi/V–O[a]	2.41(13) Å × 2

[a]Symmetry equivalent: $-x - 1/3, -y + 1/3, -z + 1/3$

at room temperature for pure $Bi_8V_2O_{17}$ is presented in Figure 1. The structure has been modelled on the single crystal parameters and clearly shows a number of reflections not accounted for by the rhombohedral model. These peaks cannot be attributed to any other phases in this system and are due to superlattice ordering. It can therefore be concluded that the refined rhombohedral structure represents the disordered substructure and that the true cell is significantly larger. The substructure model is similar to that of $BiLa_2O_5$ [19] and is fluorite related, however, full structural analysis requires optimisation of the oxygen positions within the superlattice, which is currently underway using high resolution neutron diffraction data. Nevertheless, the disordered substructure model does allow for reasonable analysis of X-ray powder diffraction data where scattering is dominated by the heavy cations.

Polycrystalline $Bi_8V_2O_{17}$ exhibits a relatively low conductivity, with values of 9.0×10^{-4} S·cm^{-1} at 600 ºC (σ_{600}) and 8.7×10^{-7} S·cm^{-1} at 300 ºC (σ_{300}). The Arrehnius plot of conductivity for $Bi_8V_2O_{17}$ is presented in Fig. 2. The data can be fitted to two linear regions above and below ca. 550 ºC, with activation energies of ΔE_{ht} = 1.09 eV and ΔE_{lt} = 1.02 eV, respectively, indicative of a phase transition. X-ray data collected at high temperature (700 ºC) reveal no obvious changes in superstructure from the pattern at ambient temperature. This may suggest that, if present, the phase transition is subtle.

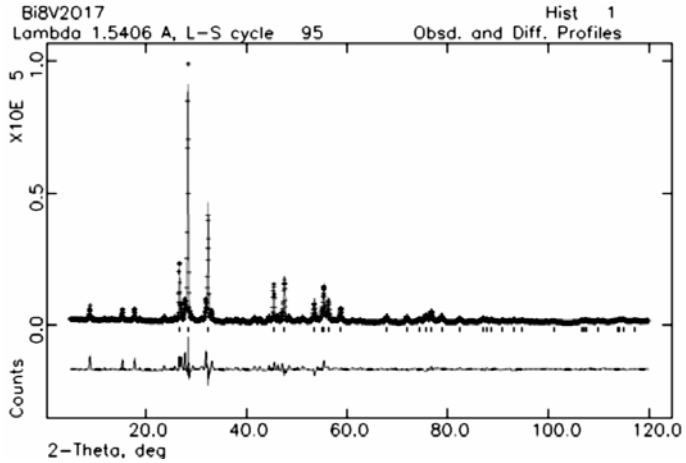

Fig. 1. Fitted X-ray diffraction pattern of polycrystalline $Bi_8V_2O_{17}$ at room temperature using rhombohedral substructure model. Observed (points) fitted (line) and difference (lower) profiles are shown. Calculated reflection positions are indicated by markers

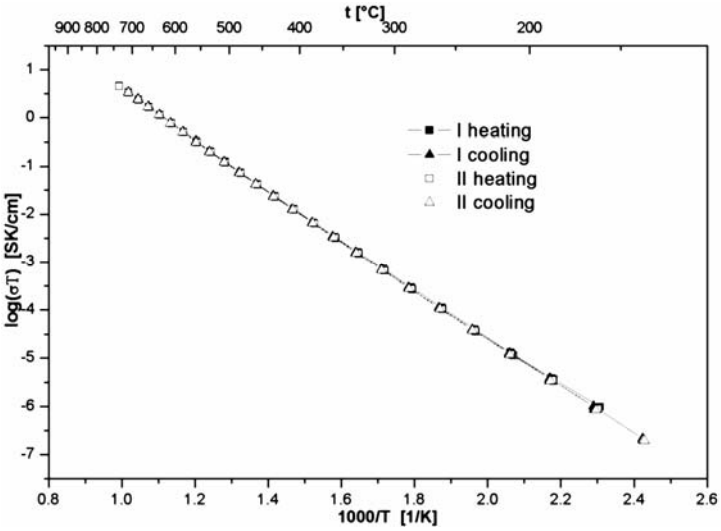

Fig. 2. Arrhenius plots of total electrical conductivity for polycrystalline $Bi_8V_2O_{17}$ over two cycles of heating and cooling

$Bi_8V_2O_{17}$ is observed as a product in the pseudo-binary system Bi_2ZrO_5–$Bi_2VO_{5.5}$ ($Bi_2Zr_xV_{1-x}O_{5.5-x/2}$) for compositions above the BIMEVOX solid solution limit [12] at around x = 0.20. At higher values of x, tetragonal γ-BIZRVOX appears along with peaks corresponding to $Bi_8V_2O_{17}$ and ZrO_2. These three phases persist up to x = 0.40, with $Bi_8V_2O_{17}$ becoming more dominant, until at x = 0.50 γ-BIZRVOX is undetectable. The variation in unit cell parameters for the $Bi_8V_2O_{17}$ type phase with composition in these samples is shown in Figure 3. The variation, particularly in the c-parameter, suggests limited solid solution formation. The electrical properties also show compositionally dependent variation. As x increases, ΔE_{ht} of the sample increases and conductivity decreases up to x = 0.50. At this composition, an Arrhenius plot of conductivity similar to that of pure $Bi_8V_2O_{17}$ is observed (Fig. 4), but with lower total conductivity (σ_{600} = 2.8 ×10^{-4} S·cm^{-1} and σ_{300} = 3.3 × 10^{-7} S·cm^{-1}). The value for the low-temperature activation energy (ΔE_{lt} = 1.01 eV) is close to that of pure $Bi_8V_2O_{17}$, however, the high temperature activation energy (ΔE_{ht} = 1.23 eV) is significantly larger than that of the pure compound.

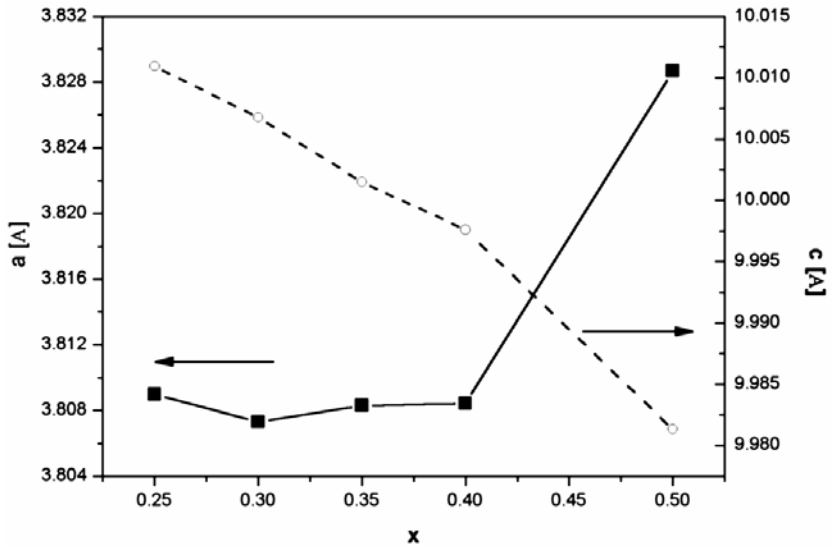

Fig. 3. Variation in $Bi_8V_2O_{17}$ unit cell parameters with composition for the polyphase system $Bi_2Zr_xV_{1-x}O_{5.5-x/2}$

A similar behaviour is also observed in the $Bi_2Mg_xV_{1-x}O_{5.5-(3x/2)}$ system at compositions above the BIMEVOX phase stabilization limit (x = 0.33 in this system) [11]. For compositions above x = 0.33, a polyphase system is observed with BIMGVOX and $Bi_8V_2O_{17}$ phases present, until at x = 0.50 the BIMEVOX phase is undetectable. MgO is not observed due to a relatively low scattering factor of this component in X-rays. In this system, the Arrhenius plot for the x = 0.50 composition (Fig. 4) is identical with that of $Bi_8V_2O_{17}$. In addition, refined unit cell parameters for the $Bi_8V_2O_{17}$ type phase at this composition (a = 3.818, c = 9.933 Å) are close to those of the pure compound.

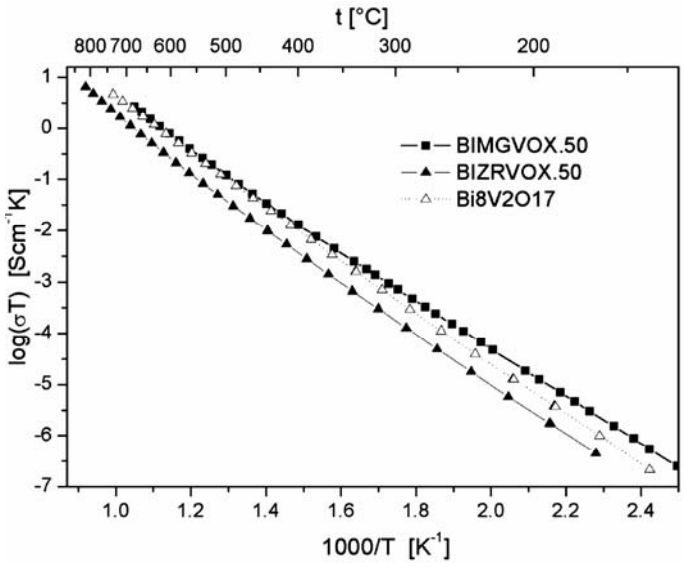

Fig. 4. Arrhenius plots of total electrical conductivity for polycrystalline $Bi_2Zr_{0.5}V_{0.5}O_{5.25}$ and $Bi_2Mg_{0.5}V_{0.5}O_{4.75}$. The plot for $Bi_8V_2O_{17}$ is included for comparison. The data correspond to the first cooling runs

4. Conclusions

$Bi_8V_2O_{17}$ appears to be a discrete stable phase in the Bi_2O_3–V_2O_5 binary system. It has a fluorite-related substructure closely resembling that of rhombohedral $BiLa_2O_5$. Electrical data appear to be consistent with a phase transition at around 550 °C.

$Bi_8V_2O_{17}$ is observed above the BIMEVOX solid solution limits in the systems $Bi_2Zr_xV_{1-x}O_{5.5-x/2}$ and $Bi_2Mg_xV_{1-x}O_{5.5-(3x/2)}$ and is the dominant phase at compositions containing a 4:1 ratio of Bi_2O_3:V_2O_5. Variation in total conductivity and unit cell parameters suggest that a limited solid solution may be formed with ZrO_2.

Acknowledgements

We gratefully acknowledge support under the EC framework 5 Centre of Excellence CEPHOMA (Contract No. ENK5-CT-2002-80666). The authors wish to thank Dr. R.M. Wilson at Queen Mary for high resolution X-ray powder diffraction data collection and M. Motevalli at Queen Mary for his assistance in single crystal data collection.

References

[1] QURASHI M.M., BARNES W.H, Amer. Mineralogist, 38 (1953), 489.
[2] COX D.E., MOODENBAUGH A.R., SLEIGHT A.W., CHEN H.Y., NBS Special Publication, 567 (1980), 189.
[3] ABRAHAM F., DEBREUILLE-GRESSE M.F., MAIRESSE G., NOWOGROCKI G., Solid State Ionics, 28–30 (1988), 529.

[4] WATANABE A., J. Solid State Chem., 161 (2001), 410.
[5] WATANABE A., KITARNI Y., Solid State Ionics, 113–115 (1998), 601.
[6] ICDD Powder Diffraction File, PDF-2, ICDD, Pennsylvania, USA, 1998, Card 44–171.
[7] LEE M.D., CHEN W.S., CHIANG H.P., Appl. Catal. A., 101 (1993), 269.
[8] ABRAHAM F., BOIVIN J.C., MAIRESSE G., NOWOGROCKI G., Solid State Ionics, 40/41 (1990), 934.
[9] VERNOCHET C., VANNIER R-N., HUVE M., PIROVANO C., NOWORGROCKI G., MAIRESSE G., VAN TENDELOO G., J. Mater. Chem., 10 (2000), 2811.
[10] LAZURE S., VANNIER R-N., NOWOGROCKI G., MARIESSE G., MULLER CH., ANNE M., STROBEL P., J. Mater. Chem., 5 (1995), 1395.
[11] ABRAHAMS I., KROK F., MALYS M., WROBEL W., CHAN S.C.M, BOGUSZ W., DYGAS J.R., Solid State Ionics, 157 (2003), 155.
[12] WROBEL W., KROK F., ABRAHAMS I., KOZANECKA A., MALYS M., BOGUSZ W., DYGAS J.R., Solid State Ionics, 175 (2004), 425
[13] NORTH A.C.T., PHILLIPS D.C., MATTHEWS F.S., Acta Crystallogr., Sect. A, 24 (1968), 351.
[14] Programs for Crystal Structure Analysis (Release (97-2), SHELDRICK G.M., Insitüt für Anorganische Chemie der Universität, Tammanstrasse 4, D-3400 Göttingen, Germany, 1998; SHELDRICK G.M., Acta Crystallogr., Sect. A, 46 (1990), 467; SHELDRICK G.M., SHELXL-93, University of Göttingen, 1993.
[15] FARRUGIA L.J., J. Appl. Cryst., 32 (1999), 837.
[16] LARSON A.C., VON DREEL R.B., Los Alamos National Laboratory, Report N^{o}. LA-UR-86-748, (1987).
[17] ABRAHAMS I., KROK F., NELSTROP J.A.G., Solid State Ionics, 90 (1996), 57.
[18] SMITH D.K., NEWKIRK H.W., Acta Crystallogr., 18 (1965), 983.
[19] WOLCYRZ M., KEPINSKI L., HORYN R., J. Solid State Chem., 116 (1995), 72.

Received 10 December 2004
Revised 12 September 2005